Editors' Suggestion

Trouble beyond H_0 and the new cosmic triangles

José Luis Bernal,[1] Licia Verde,[2,3] Raul Jimenez,[2,3] Marc Kamionkowski,[1]
David Valcin,[2] and Benjamin D. Wandelt[4,5,6]

[1]*Department of Physics and Astronomy, Johns Hopkins University, 3400 North Charles Street, Baltimore, Maryland 21218, USA*
[2]*ICC, University of Barcelona, Martí i Franquès, 1, E-08028 Barcelona, Spain*
[3]*ICREA, Passeig Lluis Companys 23, Barcelona 08010, Spain*
[4]*Sorbonne Université, CNRS, UMR 7095, Institut d'Astrophysique de Paris, 98 bis bd Arago, 75014 Paris, France*
[5]*Sorbonne Université, Institut Lagrange de Paris (ILP), 98 bis bd Arago, 75014 Paris, France*
[6]*Center for Computational Astrophysics, Flatiron Institute, 162 5th Avenue, New York, New York 10010, USA*

(Received 15 February 2021; accepted 8 April 2021; published 26 May 2021)

The distance ladder using supernovae yields higher values of the Hubble constant H_0 than those inferred from measurements of the cosmic microwave background (CMB) and galaxy surveys, a discrepancy that has come to be known as the "Hubble tension". This has motivated the exploration of extensions to the standard cosmological model in which higher values of H_0 can be obtained from CMB measurements and galaxy surveys. The trouble, however, goes beyond H_0; such modifications affect other quantities, too. In particular, their effects on cosmic times are usually neglected. We explore here the implications that measurements of the age t_U of the Universe, such as a recent inference from the age of the oldest globular clusters, can have for potential solutions to the H_0 tension. The value of H_0 inferred from the CMB and galaxy surveys is related to the sound horizon at CMB decoupling (or at radiation drag), but it is also related to the matter density and to t_U. Given this observation, we show how model-independent measurements may support or disfavor proposed new-physics solutions to the Hubble tension. Finally, we argue that cosmological measurements today provide constraints that, within a given cosmological model, represent an overconstrained system, offering a powerful diagnostic tool of consistency. We propose the use of ternary plots to simultaneously visualize independent constraints on key quantities related to H_0 like t_U, the sound horizon at radiation drag, and the matter density parameter. We envision that this representation will help find a solution to the trouble of and beyond H_0.

DOI: 10.1103/PhysRevD.103.103533

I. INTRODUCTION

The standard, ΛCDM, cosmological model, has successfully passed increased scrutiny, as observations of the cosmic microwave background (CMB) [1–3], type-Ia supernovae (SNeIa) [4] and large-scale structure [5–8] have improved drastically over recent years. Nonetheless, tensions have arisen for specific parameters when their values are inferred, within the ΛCDM, from different probes and observables. The biggest tension is related to determinations of the Hubble constant $H_0 \equiv 100h$ km/s/Mpc, and has increased in the last decade to be in the 4–5σ [9,10].

The current state of the H_0 tension is illustrated in Fig. 1, where we show marginalized posteriors for measurements depending on early-times physics (like *Planck* [1] or baryon acoustic oscillations with a big bang nucleosynthesis (BBN) prior on the physical density of baryons [11,12]), late-time expansion history (using strong lensing time delays from TDCOSMO [13–17][1] and cosmic chronometers [19,20]), and local measurements, independent of cosmology, from SH0ES [21] and CCHP [22]. Except for cosmic chronometers, all competitive H_0 constraints considered here rely on distance measurements.[2]

The two determinations yielding the largest tension are obtained from the CMB power spectra and the SH0ES distance ladders using SNeIa calibrated by Cepheids. CCHP calibrates the SNeIa instead with the tip of the red giant branch (TRGB) and finds a lower value of H_0 [22] (see also [26–28]).

[1]There are ongoing efforts to relax the dependence of strong lensing time delays H_0 inference on the assumed expansion rate [18].

[2]Some H_0 constraints related with large-scale structure do not depend on the sound horizon, but still depend on distance scales, such as the size of the horizon at matter-radiation equality [23,24].

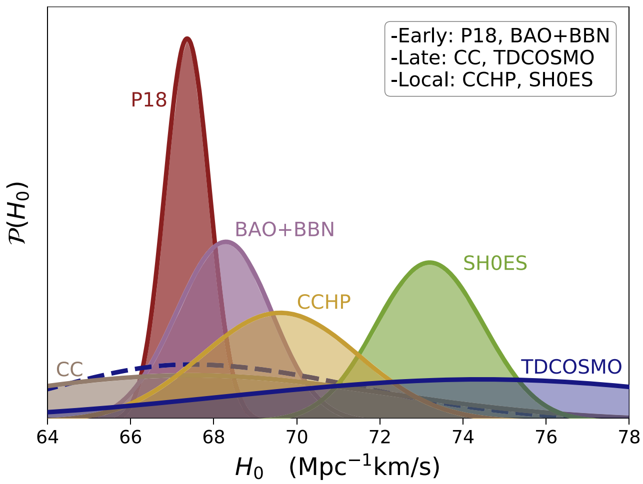

FIG. 1. Summary of constraints on H_0 from cosmic chronometers (CC) [20], *Planck* (P18) [1], baryon acoustic oscillations with a BBN prior on the baryon abundance (BAO + BBN) [12], CCHP [22], SH0ES [25], and strong-lensing time delays (TDCOSMO) [17]. We also show (dashed line) the TDCOSMO constraint including resolved kinematics from SLACS galaxies, which assumes both samples belong to the same parent population. Note that the results shown in this figure are subject to different model assumptions.

Given the strong constraints imposed by available data on the product of the sound horizon $r_{\rm d}$ at radiation drag and h, $r_{\rm d}$ has been targeted as the critical quantity to be modified in order to solve the H_0 tension. Baryon acoustic oscillations (BAO) and SNeIa disfavor any strong deviation from the evolution of the expansion rate predicted ΛCDM, while strongly constraining $r_{\rm d}h$ [29–31]. In light of current constraints, the modifications of ΛCDM best poised to reduce the H_0 tension involve altering prerecombination physics as to lower the value of $r_{\rm d}$, as it is discussed in Ref. [32], where it is argued that other possibilities, both before and after recombination are disfavored by observations or theoretically unlikely. There is a plethora of proposed models to do so and those showing more promise involve boosts of the expansion history between matter-radiation equality and recombination (see e.g., [33–48]).

Despite the fact that most of the attention has been focused on modifying distance scales across cosmic history, the expansion rate, thus H_0, also determines the age-redshift relation. Measuring cosmic ages can provide a constraint on H_0 completely independent from $r_{\rm d}$, other standard scales, or distance measurements (see e.g., [49] for a study regarding the presence of a cosmological constant). Cosmic chronometers measure directly the expansion rate using differential ages [19]; this approach is limited to relatively low redshifts, covering a range that overlaps with distance measurements. On the other hand, since relative changes in the expansion history at early times do not significantly modify the age of the Universe, independent inferences of absolute lookback times, such as the age of the Universe, may weigh in on the H_0 tension.

In this work, we discuss how the age of the Universe inferred from a recent determination of the age of the oldest globular clusters [50–52] can offer an additional perspective on the H_0 controversy. Our results suggest that an accurate and precise measurement of the age of the Universe provides an important test of the hypothesis that the H_0 tension suggests new early-Universe physics but standard late-Universe physics. In the process, we also update constraints on the low-redshift expansion rate using recent relative distance redshift measurements.

In the same way as the H_0 tension was reframed as the inconsistency between $r_{\rm d}$, h, and their product $r_{\rm d}h$ (inferred independently in a model-agnostic way from low redshifts observations) [29–31], the same can be said about other sets of quantities that can be constrained independently, albeit assuming a cosmological model. One is the combination of the matter density parameter $\Omega_{\rm M}$ today, h^2, and their product, the physical matter density $\Omega_{\rm M}h^2$. The other set is the age $t_{\rm U}$ of the Universe and h, and their combination $t_{\rm U}h$, which is completely determined by the shape of the expansion history and measured independently.

This is reminiscent of the "cosmic triangle" proposed in Ref. [53] two decades ago, where the matter, cosmological constant, and curvature density parameters are related to one another because they sum to unity. The original cosmic triangle is a ternary plot which served to visualize cosmological constraints that led to favor the (now standard) flat ΛCDM model. Here, in full analogy, we propose the use of ternary plots as diagnosis diagrams to examine the tension between cosmological quantities independently measured from different observations. Ternary plots are specially suited for this purpose, as we show for the cases of $r_{\rm d}$, $\Omega_{\rm M}$, and $t_{\rm U}$ listed above.

This article is organized as follows. We present updated constraints on the late-Universe expansion rate as a function of redshift in Sec. II; discuss the role cosmic ages play in the H_0 tension in Sec. III; present the new cosmic triangles in Sec. IV; and finally conclude in Sec. V.

II. UPDATED EXPANSION RATE CONSTRAINTS

We begin by presenting updated model-agnostic constraints on the expansion rate as a function of redshift, $E(z) \equiv H(z)/H_0$, using the latest, state-of-the-art data. These constraints on $E(z)$ are a key input for the results of Secs. III, IV, and our conclusions.

We use SNeIa observations from Pantheon [4] and BAO measurements from 6dFGRS [54], SDSS DR7 [55], BOSS [5], and eBOSS, including galaxies, quasars, and Lyman-α

forest [56–60] as relative distance indicators.[3] Note that although BAO-only analyses assume a fiducial cosmology, their results are robust to be applied to other cosmologies (see e.g., [61,63]).

Two models for $E(z)$ are examined: ΛCDM, and a parametrization using natural cubic splines, the nodes of which have a varying position, without imposing flatness, which we refer to as "generic" expansion and as such falls under what we here refer to as "model-agnostic" approach. Given its flexibility, the generic expansion shall be understood as a marginalization over cosmological models predicting a smooth $E(z)$. Other uses of this parametrization, known as flexknot, can be found in e.g., Refs. [64,65].

The free parameters for the ΛCDM case are $\{\Omega_\mathrm{M}, r_\mathrm{d}, h, M_\mathrm{SN}\}$, where M_SN is the absolute magnitude of SNeIa; on the other hand, the generic expansion needs $\{z_\mathrm{knot}^{(1,N-1)}, \boldsymbol{E}_\mathrm{knot}^{(1,N)}, \Omega_\mathrm{k}, r_\mathrm{d}, h, M_\mathrm{SN}\}$ as free parameters, where $\boldsymbol{E}_\mathrm{knot}$ are the values of $E(z)$ at the knots of the splines, located at z_knot, and Ω_k is the density parameter associated with curvature. The first and last knot are fixed at $z = 0$ and $z = 2.4$, respectively, and $E(0) = 1$ by definition. Although our results do not significantly depend on the number of knots used, we find $N = 4$ provides the best performance, allowing for as much freedom as possible but avoiding overfitting and $\mathrm{d}E/\mathrm{d}z$ changing sign too many times, and report the results obtained under this choice. We use uniform priors in all cases.

We use the public code MABEL[4] [67], to run Monte Carlo Markov chains with the sampler ZEUS [68,69][5] to constrain the shape of the expansion rate in the late-time Universe ($z \leq 2.4$) and the quantity $r_\mathrm{d}h$ with uncalibrated distance measurements from BAO and SNeIa measurements. Note that, with the data included in the analysis, h and r_d individually are completely unconstrained; only their product is constrained.

The new BAO and SNeIa data allow the constraints on the generic $E(z)$ to be extended up to $z = 2.4$, as shown in Fig. 2. The generic reconstruction yields an $E(z)$ which is consistent with the prediction of a ΛCDM model from *Planck* and BAO + SNeIa. Allowed deviations from *Planck*'s ΛCDM best fit are $\lesssim$3–4% at $z \lesssim 0.8$; this bound weakens slightly $\lesssim$10% at $0.8 \lesssim z \lesssim 2.4$, due to the degradation in the constraining power of SNeIa observations. While still being consistent with the ΛCDM

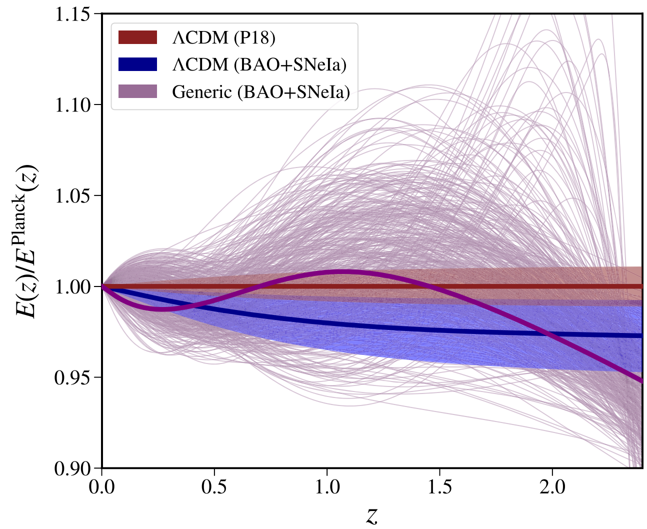

FIG. 2. Best fit evolution of the expansion rate with redshift (thick lines) normalized by *Planck*'s ΛCDM best fit $[E(z)/E^\mathrm{Planck}(z)]$ and 68% confidence level uncertainties (shaded regions, thin lines). *Planck*'s ΛCDM results are reported in red and BAO + SNeIa constraints assuming ΛCDM are in blue. In purple, the reconstruction from BAO + SNeIa assuming a generic expansion; thin lines are a sample of 500 flexknot splines reconstruction from the 68% cases with highest posterior.

prediction, the reconstructed posterior allows for a boost of the expansion rate (~15% larger than *Planck*'s ΛCDM best fit) at $1.5 \lesssim z \lesssim 2.4$, this can be seen as an "excess wiggle" in the plot; however, it is not significant and we should remark that there are no measurements in that redshift range corresponding to the gap between the redshift covered by Supernovae data/eBOSS quasars and the Lyman-α forest data. Note also that those expansion histories showing an excess expansion rate at these redshifts need a lower $E(z)$ than ΛCDM at low redshifts. These results extend and improve previous constraints from agnostic reconstructions of $E(z)$ (see e.g., Ref. [29], where reported 68% confidence level limits of the deviations are 5% at $z \lesssim 0.6$ but grow significantly at higher redshift).

Moreover, we find $\Omega_\mathrm{k} = -0.02 \pm 0.10$ and $r_\mathrm{d}h = 100.3 \pm 1.2$ Mpc which represent, respectively, a factor of 6 and factor of 2 improvement compared to the results reported in Ref. [71] [although the parametrization of $E(z)$ is different, so this comparison is more qualitative than strictly quantitative; the improvement is driven by the new data gathered over the past five years]. These constraints can be compared to those obtained also from BAO + SNeIa when assuming a flat ΛCDM model: $r_\mathrm{d}h = 100.6 \pm 1.1$ Mpc and $\Omega_\mathrm{M} = 0.297 \pm 0.013$. As can be seen, the generic reconstruction, despite having five extra model parameters, does not degrade the ΛCDM $r_\mathrm{d}h$ constraints. Furthermore, it returns constraints on $r_\mathrm{d}h$ comparable to *Planck* results assuming ΛCDM ($r_\mathrm{d}h = 99.1 \pm 0.9$ Mpc), without relying on early-time physics or observations.

[3]Standard BAO analyses adopt a prior on r_d to break the $r_\mathrm{d}h$ degeneracy and calibrate the distance measurements, following the approach known as inverse cosmic distance ladder. Not using that prior and marginalizing over r_d removes any dependence on prerecombination physics, since the BAO measurements are robust to modifications of the prerecombination physics of ΛCDM [61]. We use measurements from BAO-only analyses, following the eBOSS likelihoods and criterion to combine with BOSS measurements from [62].

[4]See Ref. [66].

[5]See Ref. [70].

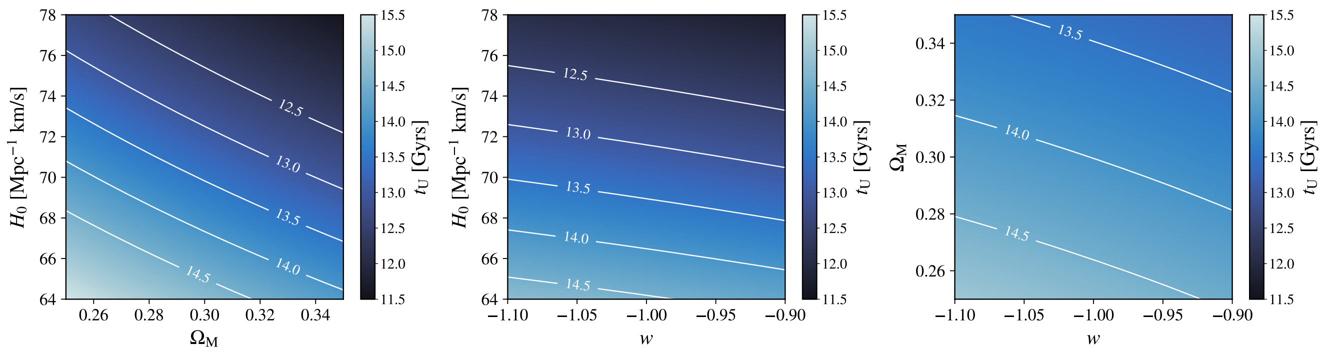

FIG. 3. Age of the Universe (in Gyr) as function of H_0 and Ω_M for $w = -1$ (left panel), H_0 and w for $\Omega_M = 0.3138$ (central panel), and Ω_M and w for $h = 0.6736$ (right panel). When a parameter is not varied, it is fixed to *Planck* ΛCDM best-fit value. White lines mark contours with constant value of t_U.

III. COSMIC AGES AND H_0

In addition to cosmic distances, the expansion rate of the Universe determines the lookback time. This opens up the possibility to use time (or age) measurements to weigh in on the H_0 tension. The cosmic chronometers method uses relative ages to determine $H(z)$, but ages can also be used in a complementary way. The lookback time t as function of redshift is given by

$$t(z) = \frac{977.8}{H_0}\int_0^z \frac{dz'}{(1+z')E(z')}\,\text{Gyr}, \tag{1}$$

with $H(z)$ in km s^{-1} Mpc^{-1}. Following Eq. (1), the age of the Universe is $t_U \equiv t(\infty)$. We show the dependence of t_U on H_0, Ω_M, and a constant equation of state parameter w for dark energy in a wCDM model in Fig. 3. It is evident that the strongest dependence is on H_0, while Ω_M and w have less influence.

The integral in Eq. (1) is dominated by contributions from redshifts below few tens, decreasing as z grows. Therefore, any exotic prerecombination physics does not significantly affect the age of the Universe. On the other hand, $E(z)$ is bound to be very close to that of a CMB-calibrated ΛCDM model at $z \lesssim 2.4$, as shown in the previous section. Hence, a precise and robust determination of t_U which does not significantly rely on a cosmological model, in combination with BAO and SNeIa, may weigh in on proposed solutions to the H_0 tension. If an independent (and model-agnostic) determination of t_U were to coincide with *Planck*'s inferred value assuming ΛCDM, ~13.8 Gyrs, alternative models involving exotic physics relevant only in the early Universe would need to invoke additional modifications also of the late-Universe expansion history to reproduce all observations with a high value of H_0 as their prediction for t_U would be too low. This is because the value of the integral in Eq. (1) assuming standard physics after recombination cannot be too different from ΛCDM's prediction once BAO and SNeIa are considered, and then $t_U \propto H_0^{-1}$. As we will see below, current measurements of t_U are just precise enough to hint at this scenario.

Recently, a value of the age of Universe, $t_U = 13.5 \pm 0.15(\text{stat.}) \pm 0.23(\text{syst.})$ (± 0.27 when adding statistical and systematic uncertainties in quadrature) was inferred from a sample of old globular clusters (GCs) in Refs. [51,52].[6] This study involves a Bayesian analysis of the properties of 38 GCs, including their age, distance, metallicity, reddening, and abundance of α-enhanced elements. t_U is inferred from the age of the oldest of these GCs (marginalized over all other parameters and including systematic errors) estimating and correcting for the age of the Universe at the moment of GCs formation, and generously marginalizing over the small residual dependence on cosmology.

We can confront local H_0 measurements with the t_U inferred from GCs, since they are related by $H_0 t_U$, which can be obtained using Eq. (1) and a constraint on $E(z)$ for all the redshifts that contribute significantly to the integral. Redshifts below 2.4 [where the generic $E(z)$ reconstruction is available] only cover about 75% of the age of the Universe. If we assume that deviations from a ΛCDM expansion history are driven by the poorly known dark energy component, then $E(z)$ at $z > 2$ is effectively that of an Einstein de Sitter Universe. In this case the reconstructed $E(z)$ is perfectly consistent with ΛCDM and only relatively small deviations are allowed. If we consider more extreme deviations from ΛCDM, additional data probing the expansion history at higher redshifts would be needed to extend the constraints on the generic $E(z)$ to cover a larger fraction of t_U.

[6]This systematic uncertainty was determined using external metallicity spectroscopic measurements of the GCs. We refer the interested reader to Ref. [52] for more details and an alternative estimate based only on the color-magnitude diagrams of the globular clusters.

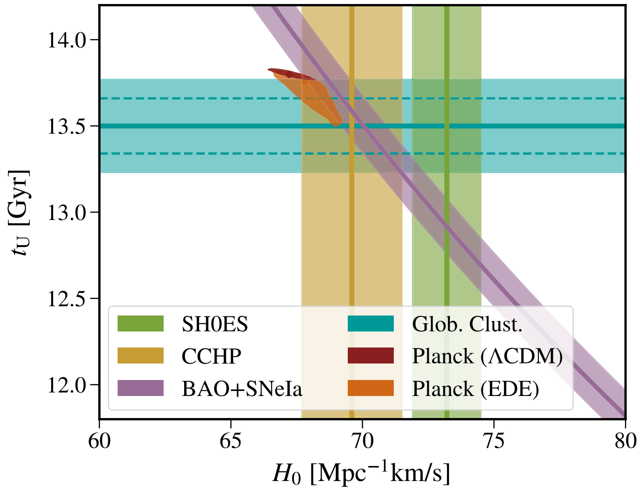

FIG. 4. 68% confidence level marginalized constraints in the H_0–t_U plane, from independent measurements, as indicated in the legend. Dashed cyan lines denote the size of the statistical 1σ errors from globular clusters, while the shaded region also includes systematic uncertainties. BAO + SNeIa constraints assume a ΛCDM cosmology. We show *Planck* results assuming ΛCDM (red) and EDE (orange).

Hence, we assume for this study a ΛCDM expansion rate $E(z)$, using the value of Ω_M inferred from BAO and SNeIa and its error.[7] Note that exotic models modifying only prerecombination cosmology do not affect directly the late-time $E(z)$ (which remains that of a ΛCDM model); hence, our inferred $H_0 t_U$ also applies to these models. As an example, we consider early dark energy (EDE) models. In particular, we use the EDE model posterior obtained in Refs. [72,73] for the *Planck* data; the model features three additional cosmological parameters compared to ΛCDM.

We show 68% confidence level marginalized constraints on the H_0–t_U plane from SH0ES, CCHP, GCs, BAO + SNeIa, and *Planck* in Fig. 4. We find $H_0 t_U = 945 \pm 11$ Gyr Mpc^{-1} km/s from BAO + SNeIa assuming ΛCDM, while $H_0 t_U = 928 \pm 7$ and 932 ± 7 Gyr Mpc^{-1} km/s from *Planck* assuming ΛCDM and EDE, respectively. As a reference, combining BAO + SNeIa with SH0ES and TRGB returns $t_U = 12.93 \pm 0.29$ and $t_U = 13.62 \pm 0.42$ Gyr, respectively, while *Planck*'s inferred values are 13.80 ± 0.02 Gyr (ΛCDM) and $13.76^{+0.06}_{-0.16}$ Gyr (EDE).

These results show that for SH0ES to be compatible with BAO + SNeIa the Universe must be significantly younger than inferred by *Planck*, no matter whether ΛCDM or EDE are assumed; this statement is robust to early-time physics assumptions. The age of the Universe inferred from GCs weakly favors older Universes than SH0ES combined with BAO + SNeIa, but the current systematic error budget is too large to firmly distinguish. There are ongoing efforts to reduce the impact of systematic errors (see e.g., [52]), so that GCs constraints on t_U have the potential to discriminate among different scenarios proposed to solve the H_0 tension (statistical errors are indicated with dashed lines).

IV. THE NEW COSMIC TRIANGLES

The H_0 tension was reframed as a consistency test between r_d (an early-time quantity) and H_0 (a late-time quantity), which can be done using a model-agnostic approach, in Ref [29]. Similarly, assuming a cosmological model, allows for a similar consistency test between Ω_M and H_0 to be performed, as proposed in Ref. [74]. With the updated constraints on $E(z)$, $r_d h$, and Ω_M obtained in Sec. II, we can revisit these consistency checks. Moreover, the H_0, t_U, and $H_0 t_U$ constraints obtained with the Ω_M values inferred from BAO + SNeIa, adds a third consistency test related with H_0.

These three cases are three triads of two cosmological quantities and their product determined independently. These triads are $\{t_U, H_0, H_0 t_U\}$, $\{r_d, h, r_d h\}$, $\{\Omega_M, h^2, \Omega_M h^2\}$. Within a given cosmological model (although some of the constraints can be obtained model independently), and in the absence of systematic errors, a generic triad $\{a, b, ab\}$ of parameters determined by independent experiments i, j, and k, respectively, is an overconstrained system which must fulfill $a_i \times b_j = (ab)_k$ within statistical uncertainty. This is what makes these triads a powerful diagnostic tool of consistency, especially in the context of the H_0 tension. Therefore, the cosmological model(s) yielding agreement of all these triads are favored by the data.

Cosmology faced a similar situation in 1999, when information from CMB anisotropies, SNeIa, and clusters observations was combined to determine whether the Universe is flat and if there was evidence for a nonzero cosmological constant [53]. In that case, the triad was $\{\Omega_M, \Omega_k, \Omega_\Lambda\}$, where $\Omega_\Lambda = 1 - \Omega_M - \Omega_k$ is the density parameter associated to the cosmological constant today.

These triads may be represented in a plane (as done e.g., in Fig. 4), but due to the relation between their components, they can be more efficiently represented in a ternary plot. Taking the logarithm of each quantity in the triads of the form $\{a, b, ab\}$ [which fulfills $\log_{10}(a) + \log_{10}(b) - \log_{10}(ab) = 0$], we can build ternary plots; every point on these ternary plots sums up to 0. This representation provides an intuitive and illustrative simultaneous look at independent cosmological constraints. We use them to illustrate the state of the H_0 tension in each of the three complementary frames that have been discussed. We refer to these ternary plots as the new cosmic triangles.

Each of the triads discussed in this work involves quantities directly related to H_0 and provides different angles to study the H_0 tension: in terms of times, distances, and the

[7]The expected effect of adopting the reconstructed $E(z)$ where available and a ΛCDM one at higher z is a possible increase of the error bars on $t_U H_0$ of $\lesssim 10\%$.

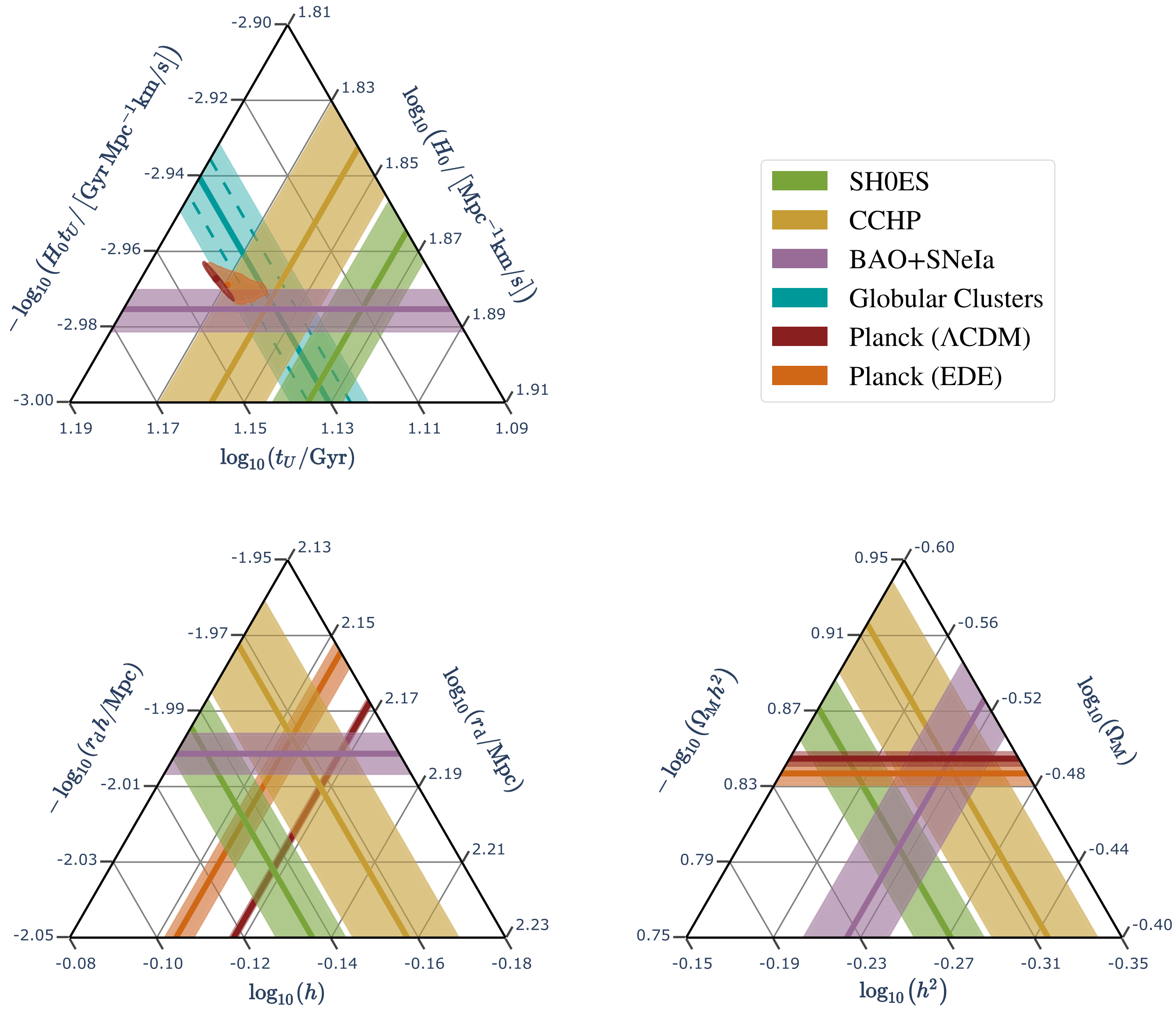

FIG. 5. 68% confidence level marginalized constraints on the new cosmic triangles: we show the triad corresponding to the age of the Universe and the Hubble constant (upper left), to the sound horizon at radiation drag and the reduced Hubble constant (bottom left), and to the total matter density parameter today and the square of the reduced Hubble constant (bottom right). Note that all points in each figure sum up to 0, while the ticks in the axes determine the direction of equal values for each axis.

abundance of matter. In interpreting the observational constraints, we can distinguish between early-time, late-time, and local observations, which in turn may depend on early-time (prerecombination), late-time (low redshift), or fully local physics. In all cases, we can use BAO + SNeIa results to link local and early-Universe measurements. Note that the triad corresponding to h and r_d is the only one that is agnostic with respect to the choice of a cosmological model for the low-redshift expansion history.[8]

[8] r_d inferred values from *Planck* are largely independent of standard postrecombination physics, as we can see comparing results from standard analyses [1] with those using only early-Universe information [71].

We show the new cosmic triangles in Fig. 5; the interpretation of the ternary plots can be eased by comparing this figure with Fig. 4. Each side of the triangle corresponds to the logarithm of one of the quantities involved, or their product, and the direction of the ticks in the axes determine the lines of equal value for each quantity. All the constraints shown in these plots (with the exception of the contours corresponding to *Planck* in the upper panel) are bands that refer only to the axis with aligned ticks. The preferred region in the parameter space will be the one with constraints from where the three axes overlap. On the other hand, if there is no point in which the constraints referring to all three axes overlap, the measurements are in tension. We can appreciate the tension within

ΛCDM in the triangles corresponding to $r_\mathrm{d}h$ and $\Omega_\mathrm{M}h^2$. As expected, considering the region favored by BAO + SNeIa, *Planck* constraints obtained within ΛCDM are consistent with CCHP, but show some tension with SH0ES. The tensions are always smaller in the case of EDE, but not enough for this model to be preferred over ΛCDM.

Figure 5 clearly shows the synergies of considering the three triads at the same time. The most studied so far has been the one involving r_d and h, since it was argued that the most promising way to solve the H_0 tension was to reduce the value r_d while keeping a standard evolution of the low-redshift expansion rate [29,32]. We can also see that this triangle is the one showing the largest tension between *Planck* assuming ΛCDM, SH0ES, and BAO + SNeIa, and the one for which models like EDE show promise. The triangle including Ω_M shows a smaller tension: combining BAO + SNeIa with SH0ES (CCHP) we find $\Omega_\mathrm{M} = 0.159 \pm 0.009$ ($\Omega_\mathrm{M} = 0.144 \pm 0.01$), which is in 1.8σ (0.1σ) tension with *Planck*'s constraint assuming ΛCDM. The tension reduces to 1.5σ when compared to the *Planck* results assuming EDE. Since BAO + SNeIa constrain $E(z)$ at low redshift to be very similar to (and fully consistent with) the best fit of *Planck* assuming ΛCDM, this tension is fully sourced by the H_0 tension, no matter the cosmological model under consideration.

However, the situation for the triad involving the age of the Universe is different. As argued above, modifications of the early-Universe cosmology do not directly change the age of the Universe. This is why *Planck* EDE posteriors overlap with those assuming ΛCDM (extending along the direction of constant Ω_M, i.e., the constraint on $H_0 t_\mathrm{U}$ from BAO + SNeIa). In this representation, the region of overlap of *Planck*, BAO + SNeIa, and GCs posteriors is in large tension with SH0ES. However, current determinations of t_U alone are not precise enough to definitively disfavor the combination of SH0ES with BAO + SNeIa.

Finally, Fig. 5 clearly indicates that if GCs were to still return a high value of t_U but with reduced error-bars, deviations from ΛCDM that only affect prerecombination physics will not be enough to reconcile all the measurements. If this will turn out to be the case, a combination of both high and low redshift modifications to the ΛCDM model may be required to solve the H_0 tension. Alternatively one would have to look into much more local effects, such as those affecting the distance ladder calibration and in particular effects or processes which may be responsible for the mismatch between CCHP and SH0ES.

V. CONCLUSIONS

The discrepancies between model-independent measurements and model-dependent inferred values of H_0 from different experiments (each of them sensitive to different physics and systematic errors) might be a hint for the need of modifying the standard ΛCDM model. The most promising deviations from ΛCDM proposed to solve such tensions involve a boost in the expansion rate before recombination, as to lower the value of r_d and reconcile the direct and the inverse distance ladder. However, we argue in this work, there is a more varied phenomenology, that goes well beyond r_d, to be matched by any new physics put forward to solve the H_0 tension, especially regarding cosmic ages: the trouble goes beyond H_0.

We update agnostic reconstructions of the evolution of the expansion rate of the late-time Universe with recent BAO and SNeIa measurements, extending the reconstruction up to $z \sim 2.4$. We find that BAO and SNeIa constrain the evolution of $H(z)$ to be fully consistent with the one from ΛCDM *Planck*'s best-fit prediction: any possible deviation must be well below the 5%(10%) level at $z < 0.8$ ($z < 2.4$). This further supports previous claims that modifications of the expansion rate at low redshifts are disfavored by the data (see e.g., [29,30,32]). In the coming years, line-intensity mapping [75–79], quasar observations [80,81], and strong lensing systems [67] will probe significantly higher redshifts, allowing for agnostic analyses like this one to be extended up to $z \sim 10$–20 (covering effectively > 90% of the Universe's history).

We discuss the impact of a recent, almost cosmology-independent, inference of the age of the Universe from the age of the oldest globular clusters. While the relation between H_0 and r_d can be addressed with modifications of the early-time physics, t_U is dominated by the expansion rate at $z \lesssim 30$, hence insensitive to high-redshift cosmology. The t_U determination is also insensitive to effects such as cosmological dimming (e.g., violations of the Etherington relation), cosmological screening, deviations from general relativity at large scales affecting growth of structures, and any phenomenology affecting cosmological distance measures. Therefore, if a high t_U were to be measured reliably and with small enough error bars, it would disfavor models with high H_0 and standard low-redshift physics. In this case then both, pre- and post-recombination modifications to ΛCDM, may be required to reconcile all measurements. Alternatively one would have to invoke much more local effects (be these cosmological, see e.g., [82–85], or astrophysical, in particular effects or processes which may be responsible for the mismatch between CCHP and SH0ES) affecting the local H_0 determination only, while leaving all other cosmological observations unchanged.

In such case, viable solutions to the H_0 trouble will fall in either of two classes of very different nature: local and global. Global solutions, would have to invoke new physics beyond ΛCDM which affect the entire Universe history from before recombination all the way to the low-redshift, late-time Universe. Modifying only early-time physics will not be enough. Because of their global nature, such solutions affect quantities well beyond H_0, but would be highly constrained by the wealth of high-precision cosmological observations available. Local solutions on the other hand, leave unaffected the global properties of cosmology; as such either do not require new physics beyond ΛCDM (and thus fall in the realm of astrophysics), or include new physics which only affect very local observations.

A program to improve the inference of t_U and reduce the systematic uncertainties, may give this measurement enough power to discriminate between these two different kinds of viable solutions for the H_0 tension.

Finally we identify three triads of independently measured quantities, relating H_0 with t_U, r_d, Ω_M, respectively. Each of these triads is an overconstrained system, hence we propose the use of ternary figures (the new cosmic triangles) to report and visualize the constraints. These new cosmic triangles allow for a simultaneous and easy-to-interpret visual representation of constraints on different yet related quantities. We hope that this representation will help to guide further efforts to find a solution to the trouble of (and beyond) H_0.

ACKNOWLEDGMENTS

The authors thank Tristan L. Smith, Vivian Poulin, and Geoff C.-F. Chen for comments on last versions of this manuscript. J. L. B. is supported by the Allan C. and Dorothy H. Davis Fellowship. This work is supported in part by MINECO Grant No. PGC2018-098866-B-I00 FEDER, UE. L. V. acknowledges support by European Union's Horizon 2020 research and innovation program ERC (BePreSySe, Grant Agreement 725327). ICC researchers acknowledge "Center of Excellence Maria de Maeztu" award to the ICCUB (CEX2019-000918-M). This work was supported at Johns Hopkins by NSF Grant No. 1818899 and the Simons Foundation. The work of B. D. W. is supported by the Labex ILP (reference ANR-10-LABX-63) part of the Idex SUPER, received financial state aid managed by the Agence Nationale de la Recherche, as part of the programme Investissements d'avenir under the reference ANR-11-IDEX-0004-02; and by the ANR BIG4 project, Grant No. ANR-16-CE23-0002 of the French Agence Nationale de la Recherche. The Center for Computational Astrophysics is supported by the Simons Foundation.

[1] N. Aghanim *et al.* (Planck Collaboration), Planck 2018 results. VI. Cosmological parameters, Astron. Astrophys. **641**, A6 (2020).

[2] J. W. Henning *et al.*, Measurements of the temperature and E-mode polarization of the CMB from 500 square degrees of SPTpol data, Astrophys. J. **852**, 97 (2018).

[3] S. Aiola, E. Calabrese, L. Maurin, S. Naess, B. L. Schmitt *et al.*, The atacama cosmology telescope: DR4 maps and cosmological parameters, arXiv:2007.07288.

[4] D. M. Scolnic, D. O. Jones, A. Rest, Y. C. Pan *et al.*, The complete light-curve sample of spectroscopically confirmed SNe Ia from pan-STARRS1 and cosmological constraints from the combined pantheon sample, Astrophys. J. **859**, 101 (2018).

[5] S. Alam and *et al.* (SDSS-III BOSS Collaboration), The clustering of galaxies in the completed SDSS-III baryon oscillation spectroscopic survey: Cosmological analysis of the DR12 galaxy sample, Mon. Not. R. Astron. Soc. **470**, 2617 (2017).

[6] T. M. C. Abbott, F. B. Abdalla, A. Alarcon, J. Aleksić, S. Allam, S. Allen *et al.*, Dark Energy Survey year 1 results: Cosmological constraints from galaxy clustering and weak lensing, Phys. Rev. D **98**, 043526 (2018).

[7] C. Heymans, T. Tröster, M. Asgari, C. Blake, H. Hildebrandt, B. Joachimi *et al.*, KiDS-1000 Cosmology: Multi-probe weak gravitational lensing and spectroscopic galaxy clustering constraints, arXiv:2007.15632.

[8] S. Alam *et al.* (eBOSS Collaboration), The completed SDSS-IV extended baryon oscillation spectroscopic survey: Cosmological implications from two decades of spectroscopic surveys at the apache point observatory, Phys. Rev. D **103**, 083533 (2021).

[9] L. Verde, P. Protopapas, and R. Jimenez, Planck and the local Universe: Quantifying the tension, Phys. Dark Universe **2**, 166 (2013).

[10] L. Verde, T. Treu, and A. G. Riess, Tensions between the early and late Universe, Nat. Astron. **3**, 891 (2019).

[11] G. E. Addison, D. J. Watts, C. L. Bennett, M. Halpern, G. Hinshaw, and J. L. Weiland, Elucidating ΛCDM: Impact of baryon acoustic oscillation measurements on the Hubble constant discrepancy, Astrophys. J. **853**, 119 (2018).

[12] N. Schöneberg, J. Lesgourgues, and D. C. Hooper, The BAO + BBN take on the Hubble tension, J. Cosmol. Astropart. Phys. 10 (2019) 029.

[13] G. C. F. Chen, C. D. Fassnacht, S. H. Suyu, C. E. Rusu, J. H. H. Chan, K. C. Wong *et al.*, A SHARP view of H0LiCOW: H_0 from three time-delay gravitational lens systems with adaptive optics imaging, Mon. Not. R. Astron. Soc. **490**, 1743 (2019).

[14] K. C. Wong, S. H. Suyu, G. C. F. Chen, C. E. Rusu, M. Millon, D. Sluse *et al.*, H0LiCOW—XIII. A 2.4 per cent measurement of H_0 from lensed quasars: 5.3σ tension between early- and late-Universe probes, Mon. Not. R. Astron. Soc. **498**, 1420 (2020).

[15] A. J. Shajib, S. Birrer, T. Treu, A. Agnello, E. J. Buckley-Geer, J. H. H. Chan *et al.*, STRIDES: A 3.9 per cent measurement of the Hubble constant from the strong lens system DES J0408-5354, Mon. Not. R. Astron. Soc. **494**, 6072 (2020).

[16] M. Millon, A. Galan, F. Courbin, T. Treu, S. H. Suyu, X. Ding *et al.*, TDCOSMO. I. An exploration of systematic uncertainties in the inference of H_0 from time-delay cosmography, Astron. Astrophys. **639**, A101 (2020).

[17] S. Birrer, A. J. Shajib, A. Galan, M. Millon, T. Treu *et al.*, TDCOSMO IV: Hierarchical time-delay cosmography—joint inference of the Hubble constant and galaxy density profiles, arXiv:2007.02941.

[18] G. C. F. Chen, C. D. Fassnacht, S. H. Suyu, A. Yıldırım, E. Komatsu, and J. L. Bernal, TDCOSMO VI: Distance measurements in time-delay cosmography under the mass-sheet transformation, arXiv:2011.06002.

[19] R. Jimenez and A. Loeb, Constraining cosmological parameters based on relative galaxy ages, Astrophys. J. **573**, 37 (2002).

[20] B. S. Haridasu, V. V. Luković, M. Moresco, and N. Vittorio, An improved model-independent assessment of the late-time cosmic expansion, J. Cosmol. Astropart. Phys. 10 (2018) 015.

[21] A. G. Riess, S. Casertano, W. Yuan, L. M. Macri, and D. Scolnic, Large magellanic cloud cepheid standards provide a 1% foundation for the determination of the Hubble constant and stronger evidence for physics beyond ΛCDM, Astrophys. J. **876**, 85 (2019).

[22] W. L. Freedman, B. F. Madore, T. Hoyt, I. S. Jang, R. Beaton, M. G. Lee, A. Monson, J. Neeley, and J. Rich, Calibration of the tip of the red giant branch, Astrophys. J. **891**, 57 (2020).

[23] E. J. Baxter and B. D. Sherwin, Determining the Hubble constant without the sound horizon scale: Measurements from CMB lensing, Mon. Not. R. Astron. Soc. **501**, 1823 (2020).

[24] O. H. E. Philcox, B. D. Sherwin, G. S. Farren, and E. J. Baxter, Determining the Hubble constant without the sound horizon: Measurements from galaxy surveys, Phys. Rev. D **103**, 023538 (2021).

[25] A. G. Riess, S. Casertano, W. Yuan, J. B. Bowers, L. Macri, J. C. Zinn, and D. Scolnic, Cosmic distances calibrated to 1% precision with Gaia EDR3 parallaxes and Hubble space telescope photometry of 75 Milky Way cepheids confirm tension with LambdaCDM, Astrophys. J. Lett. **908**, L6 (2021).

[26] W. Yuan, A. G. Riess, L. M. Macri, S. Casertano, and D. M. Scolnic, Consistent calibration of the tip of the red giant branch in the large magellanic cloud on the hubble space telescope photometric system and a redetermination of the Hubble constant, Astrophys. J. **886**, 61 (2019).

[27] M. J. Reid, D. W. Pesce, and A. G. Riess, An improved distance to NGC 4258 and its implications for the Hubble constant, Astrophys. J. Lett. **886**, L27 (2019).

[28] D. M. Nataf, S. Cassisi, L. Casagrande, and A. G. Riess, On the color-metallicity relation of the red clump and the reddening toward the magellanic clouds, Astrophys. J. **910**, 121 (2021).

[29] J. L. Bernal, L. Verde, and A. G. Riess, The trouble with H_0, J. Cosmol. Astropart. Phys. 10 (2016) 019.

[30] V. Poulin, K. K. Boddy, S. Bird, and M. Kamionkowski, Implications of an extended dark energy cosmology with massive neutrinos for cosmological tensions, Phys. Rev. D **97**, 123504 (2018).

[31] K. Aylor, M. Joy, L. Knox, M. Millea, S. Raghunathan, and W. L. Kimmy Wu, Sounds discordant: Classical distance ladder and ΛCDM-based determinations of the cosmological sound horizon, Astrophys. J. **874**, 4 (2019).

[32] L. Knox and M. Millea, Hubble constant hunter's guide, Phys. Rev. D **101**, 043533 (2020).

[33] T. Karwal and M. Kamionkowski, Dark energy at early times, the Hubble parameter, and the string axiverse, Phys. Rev. D **94**, 103523 (2016).

[34] V. Poulin, T. L. Smith, T. Karwal, and M. Kamionkowski, Early Dark Energy can Resolve the Hubble Tension, Phys. Rev. Lett. **122**, 221301 (2019).

[35] T. L. Smith, V. Poulin, and M. A. Amin, Oscillating scalar fields and the Hubble tension: A resolution with novel signatures, Phys. Rev. D **101**, 063523 (2020).

[36] M.-X. Lin, G. Benevento, W. Hu, and M. Raveri, Acoustic dark energy: Potential conversion of the Hubble tension, Phys. Rev. D **100**, 063542 (2019).

[37] P. Agrawal, F.-Y. Cyr-Racine, D. Pinner, and L. Randall, Rock 'n' roll solutions to the Hubble tension, arXiv:1904.01016.

[38] K. V. Berghaus and T. Karwal, Thermal friction as a solution to the Hubble tension, Phys. Rev. D **101**, 083537 (2020).

[39] J. Sakstein and M. Trodden, Early Dark Energy from Massive Neutrinos as a Natural Resolution of the Hubble Tension, Phys. Rev. Lett. **124**, 161301 (2020).

[40] F. Niedermann and M. S. Sloth, New early dark energy, Phys. Rev. D **103**, L041303 (2021).

[41] M. Zumalacárregui, Gravity in the era of equality: Towards solutions to the Hubble problem without fine-tuned initial conditions, Phys. Rev. D **102**, 023523 (2020).

[42] M. Braglia, M. Ballardini, W. T. Emond, F. Finelli, A. E. Gümrükçüoğlu, K. Koyama, and D. Paoletti, Larger value for H_0 by an evolving gravitational constant, Phys. Rev. D **102**, 023529 (2020).

[43] M. Ballardini, M. Braglia, F. Finelli, D. Paoletti, A. A. Starobinsky, and C. Umiltà, Scalar-tensor theories of gravity, neutrino physics, and the H_0 tension, J. Cosmol. Astropart. Phys. 10 (2020) 044.

[44] M. Braglia, W. T. Emond, F. Finelli, A. E. Gumrukcuoglu, and K. Koyama, Unified framework for early dark energy from α-attractors, Phys. Rev. D **102**, 083513 (2020).

[45] G. Ballesteros, A. Notari, and F. Rompineve, The H_0 tension: Δ G_N vs Δ $N_{\rm eff}$, J. Cosmol. Astropart. Phys. 11 (2020) 024.

[46] F. Niedermann and M. S. Sloth, Resolving the Hubble tension with new early dark energy, Phys. Rev. D **102**, 063527 (2020).

[47] M. Braglia, M. Ballardini, F. Finelli, and K. Koyama, Early modified gravity in light of the H_0 tension and LSS data, Phys. Rev. D **103**, 043528 (2021).

[48] T. Abadi and E. D. Kovetz, Can conformally invariant modified gravity solve the Hubble tension? Phys. Rev. D **103**, 023530 (2021).

[49] A. Jaffe, H 0 and odds on cosmology, Astrophys. J. **471**, 24 (1996).

[50] R. Jimenez, A. Cimatti, L. Verde, M. Moresco, and B. Wandelt, The local and distant Universe: Stellar ages and H_0, J. Cosmol. Astropart. Phys. 03 (2019) 043.

[51] D. Valcin, J. L. Bernal, R. Jimenez, L. Verde, and B. D. Wandelt, Inferring the age of the universe with globular clusters, J. Cosmol. Astropart. Phys. 12 (2020) 002.

[52] D. Valcin, R. Jimenez, L. Verde, J. L. Bernal, and B. D. Wandelt, The age of the universe with globular clusters: Reducing systematic uncertainties, arXiv:2102.04486.

[53] N. A. Bahcall, J. P. Ostriker, S. Perlmutter, and P. J. Steinhardt, The cosmic triangle: Revealing the state of the universe, Science **284**, 1481 (1999).

[54] F. Beutler, C. Blake, M. Colless, D. H. Jones, L. Staveley-Smith, L. Campbell, Q. Parker, W. Saunders, and F. Watson, The 6dF galaxy survey: Baryon acoustic oscillations and the local Hubble constant, Mon. Not. R. Astron. Soc. **416**, 3017 (2011).

[55] A. J. Ross, L. Samushia, C. Howlett, W. J. Percival, A. Burden, and M. Manera, The clustering of the SDSS DR7 main Galaxy sample—I. A 4 per cent distance measure at $z = 0.15$, Mon. Not. R. Astron. Soc. **449**, 835 (2015).

[56] H. Gil-Marín, J. E. Bautista, R. Paviot, M. Vargas-Magaña, S. de la Torre, S. Fromenteau *et al.*, The completed SDSS-IV extended baryon oscillation spectroscopic survey: Measurement of the BAO and growth rate of structure of the luminous red galaxy sample from the anisotropic power spectrum between redshifts 0.6 and 1.0, Mon. Not. R. Astron. Soc. **498**, 2492 (2020).

[57] A. Raichoor, A. de Mattia, A. J. Ross, C. Zhao, S. Alam, S. Avila *et al.*, The completed SDSS-IV extended baryon oscillation spectroscopic survey: Large-scale structure catalogues and measurement of the isotropic BAO between redshift 0.6 and 1.1 for the emission line galaxy sample, Mon. Not. R. Astron. Soc. **500**, 3254 (2020).

[58] J. Hou, A. G. Sánchez, A. J. Ross, A. Smith, R. Neveux, J. Bautista *et al.*, The completed SDSS-IV extended baryon oscillation spectroscopic survey: BAO and RSD measurements from anisotropic clustering analysis of the Quasar Sample in configuration space between redshift 0.8 and 2.2, Mon. Not. R. Astron. Soc. **500**, 1201 (2021).

[59] R. Neveux, E. Burtin, A. de Mattia, A. Smith, A. J. Ross, J. Hou *et al.*, The completed SDSS-IV extended baryon oscillation spectroscopic survey: BAO and RSD measurements from the anisotropic power spectrum of the Quasar sample between redshift 0.8 and 2.2, Mon. Not. R. Astron. Soc. **499**, 210 (2020).

[60] H. du Mas des Bourboux, J. Rich, A. Font-Ribera, V. de Sainte Agathe, J. Farr, T. Etourneau *et al.*, The completed SDSS-IV extended baryon oscillation spectroscopic survey: Baryon acoustic oscillations with Lyman-α forests, Astrophys. J. **901**, 153 (2020).

[61] J. L. Bernal, T. L. Smith, K. K. Boddy, and M. Kamionkowski, Robustness of baryon acoustic oscillations constraints to beyond-ΛCDM cosmologies, Phys. Rev. D **102**, 123515 (2020).

[62] https://svn.sdss.org/public/data/eboss/DR16cosmo/tags/v1_0_0/likelihoods/BAO-only/.

[63] P. Carter, F. Beutler, W. J. Percival, J. DeRose, R. H. Wechsler, and C. Zhao, The impact of the fiducial cosmology assumption on BAO distance scale measurements, Mon. Not. R. Astron. Soc. **494**, 2076 (2020).

[64] J. A. Vázquez, M. Bridges, M. P. Hobson, and A. N. Lasenby, Model selection applied to reconstruction of the primordial power spectrum, J. Cosmol. Astropart. Phys. 06 (2012) 006.

[65] M. Millea and F. Bouchet, Cosmic microwave background constraints in light of priors over reionization histories, Astron. Astrophys. **617**, A96 (2018).

[66] https://github.com/jl-bernal/MABEL.

[67] G. C.-F. Chen and J. L. Bernal (to be published).

[68] M. Karamanis and F. Beutler, zeus: A Python implementation of the ensemble slice sampling method (to be published).

[69] M. Karamanis and F. Beutler, Ensemble slice sampling, arXiv:2002.06212.

[70] https://zeus-mcmc.readthedocs.io/.

[71] L. Verde, J. L. Bernal, A. F. Heavens, and R. Jimenez, The length of the low-redshift standard ruler, Mon. Not. R. Astron. Soc. **467**, 731 (2017).

[72] R. Murgia, G. F. Abellán, and V. Poulin, The early dark energy resolution to the Hubble tension in light of weak lensing surveys and lensing anomalies, Phys. Rev. D **103**, 063502 (2021).

[73] T. L. Smith, V. Poulin, J. L. Bernal, K. K. Boddy, M. Kamionkowski, and R. Murgia, Early dark energy is not excluded by current large-scale structure data, arXiv:2009.10740.

[74] W. Lin, K. J. Mack, and L. Hou, Investigating the Hubble constant tension: Two numbers in the standard cosmological model, Astrophys. J. Lett. **904**, L22 (2020).

[75] K. S. Karkare and S. Bird, Constraining the expansion history and early dark energy with line intensity mapping, Phys. Rev. D **98**, 043529 (2018).

[76] J. B. Muñoz, A Standard Ruler at Cosmic Dawn, Phys. Rev. Lett. **123**, 131301 (2019).

[77] J. L. Bernal, P. C. Breysse, H. Gil-Marín, and E. D. Kovetz, User's guide to extracting cosmological information from line-intensity maps, Phys. Rev. D **100**, 123522 (2019).

[78] J. L. Bernal, P. C. Breysse, and E. D. Kovetz, Cosmic Expansion History from Line-Intensity Mapping, Phys. Rev. Lett. **123**, 251301 (2019).

[79] M. B. Silva, E. D. Kovetz, G. K. Keating, A. Moradinezhad Dizgah, M. Bethermin, P. Breysse *et al.*, Mapping large-scale-structure evolution over cosmic times, arXiv:1908.07533.

[80] G. Risaliti and E. Lusso, A Hubble diagram for quasars, Astrophys. J. **815**, 33 (2015).

[81] G. Risaliti and E. Lusso, Cosmological constraints from the Hubble diagram of quasars at high redshifts, Nat. Astron. **3**, 272 (2019).

[82] H. Desmond, B. Jain, and J. Sakstein, Local resolution of the Hubble tension: The impact of screened fifth forces on the cosmic distance ladder, Phys. Rev. D **100**, 043537 (2019).

[83] H. Desmond, B. Jain, and J. Sakstein, Erratum: Local resolution of the Hubble tension: The impact of screened fifth forces on the cosmic distance ladder [Phys. Rev. D **100**, 043537 (2019)], Phys. Rev. D **101**, 069904 (2020).

[84] H. Desmond, B. Jain, and J. Sakstein, Erratum: Local resolution of the Hubble tension: The impact of screened fifth forces on the cosmic distance ladder [Phys. Rev. D **100**, 043537 (2019)], Phys. Rev. D **101**, 129901 (2020).

[85] H. Desmond and J. Sakstein, Screened fifth forces lower the TRGB-calibrated Hubble constant too, Phys. Rev. D **102**, 023007 (2020).